EXPERIMENTAL AND NUMERICAL INVESTIGATION OF A TURBULENT JET FLOW IN AN ENCLOSURE

Rüdiger Schwarze, Jens Klostermann, Daniel Bauer and Christoph Brücker
Institut für Mechanik und Fluiddynamik,
Technische Universität Bergakademie Freiberg
Lampadiusstr. 4, D-09596 Freiberg, Germany
Ruediger.Schwarze@imfd.tu-freiberg.de

INTRODUCTION

Turbulent flows in complex geometries often exhibit an oscillating behavior of large coherent structures, even in the case of steady state boundary conditions. Recently, numerous efforts have been made to resolve these oscillations by means of numerical simulations. Unfortunately, large-eddy simulations (LES) are often very time- and memory-consuming in the case of complex flows. Therefore, the unsteady RANS (URANS) approach is an attractive alternative, especially when numerical simulations are used as a design and optimization tool. Actually, most URANS validation studies have been performed with semi-confined or unconfined flows past circular or sharpe-edged cylinders (Johannson et al., 1993; Durbin, 1995; Iaccarino et al., 2003; Catalano et al., 2003; Saghafian et al., 2003; Johansen et al., 2004; Holloway et al., 2004; Senocak et al., 2005; De and Dalal, 2006). For URANS simulations in enclosures, which are also of fundamental importance for many technical problems (Schwarze, 2006), there is no corresponding basic benchmark problem.

In the paper, a turbulent jet flow in a cavity is proposed as a new benchmark test of the URANS method. The dimensions of flow geometry under investigation are displayed in figure 1. The center of the inlet pipe is located at $x_1 = 0.125\,m$, $x_2 = 0.125\,m$, the center of the outlet pipe is located at $x_1 = 0.875\,m$, $x_2 = 0.125\,m$.

Figure 2 shows basic features of the cavity flow: (1) jet flow downstream of the inlet pipe, (2), (3) recirculating regions around the jet and (4) mean flow towards the outlet. Results from experimental measurements and corresponding numerical calculations with URANS and LES simulations are presented.

EXPERIMENT

Water model facility

The main component of the experimental facility is the cavity made of perspex. The model is fed by a closed water circuit. The flow rate in the model is tuned by a valve between $\dot{V} = 1.6 \ldots 2.2\,l/s$, which correspond to jet flow Reynolds numbers $Re_j = 7,5 \cdot 10^4 \ldots 1 \cdot 10^5$ and to bulk cross flow Reynolds numbers $Re_{cf} = 6400 \ldots 8800$.

Velocity data inside the cavity are obtained by a LDA (2D Dantec Dynamics) system. These measurements are performed on a $10\,mm \times 10\,mm$ grid in different locations in the model. Figure 3 shows the set-up for the grid on a vertical plane near to the sidewall of the cavity.

The pressure is measured by a pressure tube (orifice diameter 3 mm) connected to a pressure transducer (Kistler). Time series of the pressure were recorded at different locations within the cavity, table 1.

Table 1: Locations of pressure measurements in the cavity.

Name	$x\,[mm]$	$y\,[mm]$	$z\,[mm]$
PM1	50	50	200
PM2	500	250	200
PM3	750	250	120

Results

Profiles of the mean velocities are given later. An example of a time record of the pressure is given in figure 4. The regular oscillating behavior of the pressure is evident, the oscillations can be clearly distinguished from the smaller turbulent fluctuations.

Similar time series of pressure measurements at different locations and flow rates are analyzed by means of Fast Fourier transforms (FFT). Exemplary results are given in figures 5 and 6. Figure 5 shows FFT sprectra of the pressure at PM2, which are obtained for two different flow rates. Outstanding peaks are evident at $f_p \sim 0.15\,Hz$ in both spectra. They correspond to the coherent pressure oscillations. Turbulent pressure fluctuations are found in the inertial and the dissipation subrange. The scaling behavior for the inertial subrange ($f^{-5/3}$) and the dissipation subrange (f^{-7}) are indicated in the spectra, too.

Figure 6 gives the spectra, which are obtained for a constant flow rate in PM1 and PM3. Again, clear peaks are found at $f_p \sim 0.15\,Hz$ in both spectra. Comparing the spectra in PM1 and PM3, it is found that turbulence is decaying from PM1 to PM3, because the dissipation subrange is shifted towards smaller frequencies in PM3.

NUMERICAL MODEL

Theory

The model equations for the LES and the URANS approach are formally equivalent

$$\frac{\partial \overline{u}_i}{\partial x_i} = 0 \qquad (1)$$

$$\frac{\partial \overline{u}_i}{\partial t} + \frac{\partial}{\partial x_j}\left(\overline{u}_j \overline{u}_i\right) = -\frac{1}{\rho}\frac{\partial \overline{p}}{\partial x_i} + \nu \frac{\partial^2 \overline{u}_i}{\partial x_j^2} + \frac{\partial \tau_{ij}}{\partial x_j} \qquad (2)$$

In case of LES, the model equations are obtained from a spatial filtering procedure, which is applied implicitely to the basic flow equations. The unknown sugrid-scale stresses τ_{ij} in equation (2) are approximated by the well-known Smagorinsky subrid-scale model.

The URANS equations are obtained from an ensemble averaging procedure, which is again implicitely applied to the basic flow equations. Here, the unknown Reynolds stresses τ_{ij} in equation (2) are provided by a Reynolds stress model (RS) or alternatively Boussinesq hypothesis in combination with the standard k-ε model (KE).

Wall functions are employed in order to describe the near-wall regions in both the LES and the URANS simulations. The boundary conditions of the numerical simulations fit to the parameters of the experimental configuration. Here it has to be emphasized that the boundary conditions are steady-state conditions even in the unsteady simulation. Initial values for this flow field are taken from the corresponding steady-state solution (RANS) of the model equations.

Numerics

The model equations are solved by the finite-volume method. The numerical schemes are bounded CDS interpolation in LES and QUICK upwind interpolation in URANS simulations, CDS differencing and second-order BDF for the time integration. The solution domain contains $1.1 \cdot 10^6$ (LES) and $2.2 \cdot 10^5$ (URANS) hexahedral grid cells.

The LES simulation is performed with a time step width $\Delta t_{LES} = 0.001\,s$, a flow time intervall $\tau_{LES} = 8\,s$ is resolved in this simulation. The URANS simulations are performed with time step widths $\Delta t_{URANS} = 0.025\,s$, a flow time intervall $\tau_{URANS} = 100\,s$ are resolved in these simulations.

Results

Figure 7 displays streamlines which start in a horizontal surface at $x_3 = 0.24\,m$ just below the cavity lid in the URANS simulations. The time interval between the three subfigures is $1\,s$. The inlet pipe is located left hand side in the figures.

Due to the action of recirculating regions, the upwelling flow at the walls is directed towards the centerline of the cavity. On the right side of the inlet pipe, the wake region can be identified. The unsteady behavior of the wake flow is evident. Large vortex structures exists, which oscillate around the tundish centreline. Corresponding observations are made at the water model experiment, too.

FFT spectra from time series of velocity data obtained from the LES and the URANS simulation with the RS model are given in figures 8 and 9. The URANS simulations with the KE model do not show convergence towards a fixed peak frequency in the spectra.

Figure 8 gives the FFT spectrum of $\overline{u}_2$ which is recorded during the URANS simulation in position PM2. Similar to the spectra from the pressure measurements, a peak frequency $f_p \simeq 0.15\,Hz$ is found in the velocity time record. Not surprisingly, the inertial and dissipation subrange of the turbulence spectrum are not resolved. This finding is due to the turbulence model, which should remove all turbulent fluctuations from the velocity data.

Figure 9 gives FFT spectra of $\overline{u}_1$ and $\overline{u}_2$, which are obtained from the LES simulations. Here, no peak is found in the low frequency part of the spectra, because the resolved flow time intervall is too short ($8\,s$). On the other hand, the inertial and the dissipation subrange of the turbulence spectra are resolved. Here, dissipation is due to the action of the subgrid-scale stress model. Surprisingly, the dissipation subrange is located at frequencies above $10\,Hz$ in both spectra, whereas dissipation starts at frequencies below $10\,Hz$ in all spectra from the pressure measurements. The reason for these findings are not clear yet, it is assumed that the strong recirculating behavior of the flow is responsible for these differences.

Table 2: Strouhal numbers for different flow rates in the cavity.

$\dot{V}\,[l/s]$	St_{exp}	St_{sim}
1.6	0.16	0.17
2.1	0.13	0.18

COMPARISON

Profiles

Figures 10 to 13 show profiles of the mean and rms values of velocity data along longitudinal and lateral baselines in the cavity. In the figures, data from the LDA measurements (EXP), URANS simulations with the Reynolds stress (RS) and the k-ϵ (KE) model and finally the LES simulations (LES) are compared.

Figures 10 and 11 display the mean ($\overline{u}_{1,m}$) and the rms ($\overline{u}_{1,rms}$) values of the longitudinal velocity $\overline{u}_1$ along a longitudinal horizontal baseline in the cavity centreplane. The core of the inlet jet can be identified at $x_1 = 0.125\,m$. Both experimental and numerical data show a crossflow through the jet, i. e. $\overline{u}_1 > 0$ for $0 < x_1 \leq 0.35\,m$. Then a backflow is found, $\overline{u}_1 < 0$ for $x_1 > 0.35\,m$. Regarding the different numerical appoaches, it is found that LES fits best to the experimental data in the jet dominated region ($0 < x_1 \leq 0.15\,m$). The wake region past the jet is ($0.15\,m < x_1 \leq 0.35\,m$) is best resolved in RS. Here, LES overpredicts $\overline{u}_1$ markedly. KE is found to overestimate the length of the wake region strongly. The velocity profile of the backflow is well resolved in all numerical simulations.

For the rms profiles $\overline{u}_{1,rms}$, it is found that all simulations give a resonable prediction of the jet shear layer profiles at $x_1 = 0.12\,m$ and $x_1 = 0.15\,m$. In the wake, LES gives the best resolution of the rms profile, whereas KE underpredicts and RS overestimates the rms values. In the backflow, all simulations are in good agreeement with the experiment.

Figures 12 and 13 display the mean ($\overline{u}_{3,m}$) and the rms ($\overline{u}_{3,rms}$) values of the vertical velocity $\overline{u}_3$ along a lateral horizontal baseline which intersects the center of the inlet jet. Figure 12 shows $\overline{u}_{3,m}$, the jet shape can be clearly identified. In the jet core, both URANS simulations RS and KE overestimate $\overline{u}_{3,m}$ slightly, whereas LES underestimates $\overline{u}_{3,m}$ significantly. In the shear layers and the outer parts of the profiles, the experimental and numerical results are in good agreement. Figure 13 gives the corresponding profiles of $\overline{u}_{3,rms}$. Again, the agreement between experimental and numerical data is good in the outer parts. In the jet shear layers, LES fits best to the experiment. Here, RS overpredicts the peak values, whereas KE underestimates the rms values significantly.

Oscillations

The resulting peak frequencies of the pressure measurements and the URANS simulations with the RS model are compared in table 2. The Strouhal number St is defined as

$$St = \frac{f_p\,d}{u_{cf}} = \frac{f_p\,d\,A}{\dot{V}} \tag{3}$$

where d is the jet diameter at the pipe inlet exit and u_{cf}

is the crossflow velocity defined as the ratio of the flow rate and the cross section area $A = 0.25\,m \times 0.25\,m$ of the cavity.

It is found, that St_{exp} decreases slightly with increasing flow rate in the experiments. Contrary, St_{num} remains nearly constant in the URANS simulations. However, numerical simulations fit resonable well the experimental observations.

CONCLUSIONS

Long-term oscillating flows in continuous casting tundishes are investigated by a model experiment as well as by large eddy and URANS simulations. The results of the simulations fit well to the experimental observations (mean flow data and frequencies). Especially, long-term oscillations of the tundish flow are resolved by the URANS simulations.

However, some differences between measurements, large eddy simulations and URANS simulations are found. The large eddy simulations do not match the transition from the inertial to the dissipation subrange in turbulence spectra of the wake-flow regions correctly. The URANS simulations do not resolve a minor dependency between the Strouhal and the Reynolds number of the flow.

Therefore, refined investigations are necessary in the future in order to clarify the reasons for these shortcomings and to improve the numerical models.

REFERENCES

Johannson, S. H., Davidson, L., and Olsson, E., 1993, "Numerical simulation of vortex shedding past triangular cylinders at high Reynolds number using a k-e turbulence model", *International Journal for Numerical Methods in Fluids*, Vol. 16, pp. 859-878.

Durbin, P. A., 1995, "Separated flow computations with k-e-v2 model", *AIAA Journal*, Vol. 33, pp. 659-664.

Iaccarino, G., Ooi, A., Durbin, P. A., and Behnia, M., 2003, "Reynolds averaged simulation of unsteady separated flow", *International Journal of Heat and Fluid Flow*, Vol. 24, pp. 147-156.

Catalano, P., Wang, M., Iaccarino, G., and Moin, P., 2003, "Numerical simulation of the flow around a circular cylinder at high Reynolds numbers", *International Journal of Heat and Fluid Flow*, Vol. 24, pp. 463-469.

Saghafian, M., Stansby, P. K., Saidi, M. S., and Apsley, D. D., 2003, "Simulation of turbulent flows around a cicular cylinder using nonlinear eddy-viscosity modeling: steady and oscillatory ambient flows", *Journal of Fluids and Structures*, Vol. 17, pp. 1213-1236.

Johansen, S. T., Wu, J., and Shyy, W., 2004, "Filter-based unsteady RANS computations", *International Journal of Heat and Fluid Flow*, Vol. 25, pp. 10-21.

Holloway, D. S., Walters, K. D., and Leylek, J. H., 2004, "Prediction of unsteady, separated boundary layer over a blunt body for laminar, turbulent, and transitional flow", *International Journal for Numerical Methods in Fluids*, Vol. 45, pp. 1291-1315.

Senocak, I., Shyy, W., and Johansen, S. T., 2005, "Statistical characteristics of unsteady Reynolds-averaged Navier-Stokes simulations", *Numerical Heat Transfer B*, Vol. 46, pp. 1-18.

De, A. K., and Dalal, A., 2006, "Numerical simulation of unconfined flow past a triangular cylinder", *International Journal for Numerical Methods in Fluids*, Vol. 52, pp. 801-821.

Schwarze, R., 2006, "Unsteady RANS simulation of oscillating mould flows", *International Journal for Numerical Methods in Fluids*, Vol. 52, pp. 883-902.

FIGURES

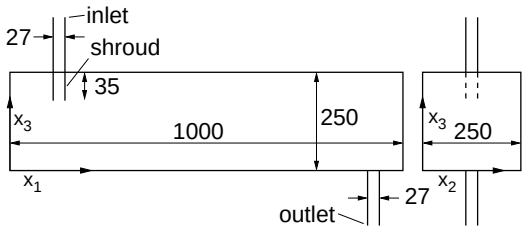

Figure 1: Dimensions of the cavity given in mm.

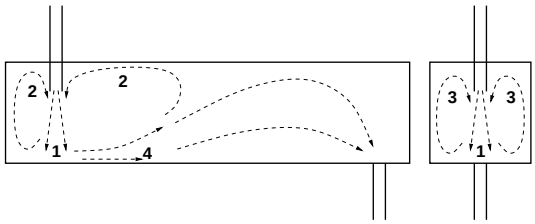

Figure 2: Basic flow structure in the cavity.

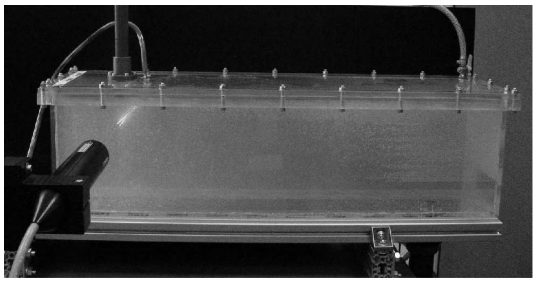

Figure 3: Water model facility.

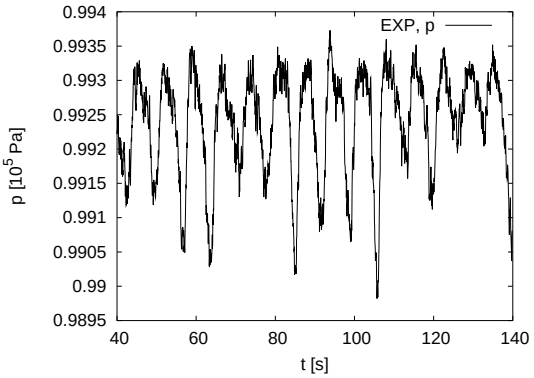

Figure 4: Example for time series of p.

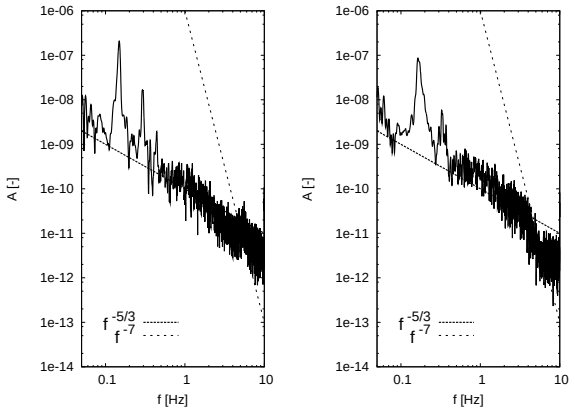

Figure 5: FFT spectra in location PM2, flow rate $\dot{V} = 1.6\,l/s$ (left) and $\dot{V} = 1.88\,l/s$ (right)

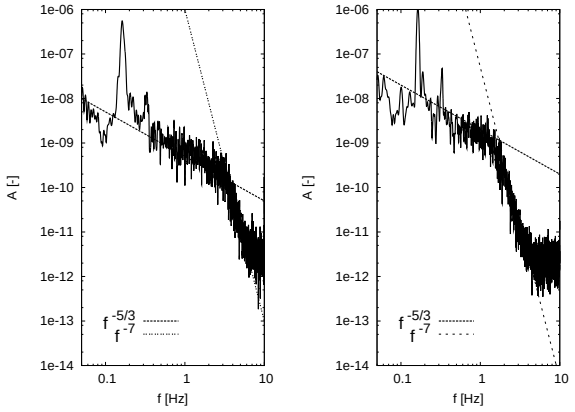

Figure 6: FFT spectra for flow rate $\dot{V} = 2.1\,l/s$ in location PM1 (left) and PM3 (right)

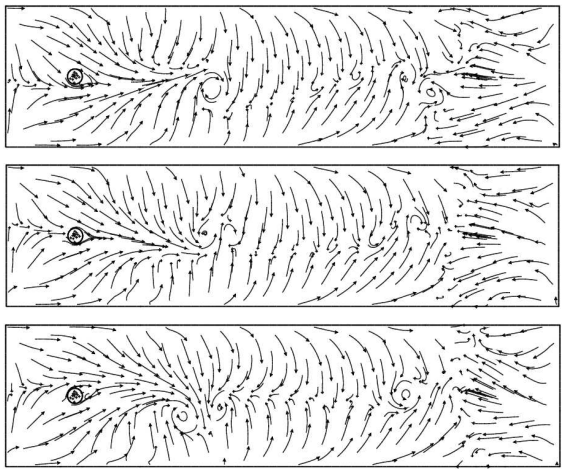

Figure 7: Streamlines for four different times in the URANS simulation

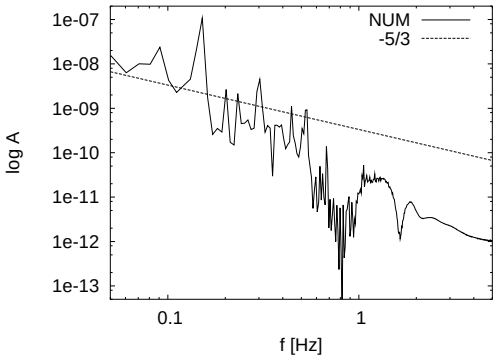

Figure 8: FFT spectra from URANS data of $\overline{u}_2$ in PM2

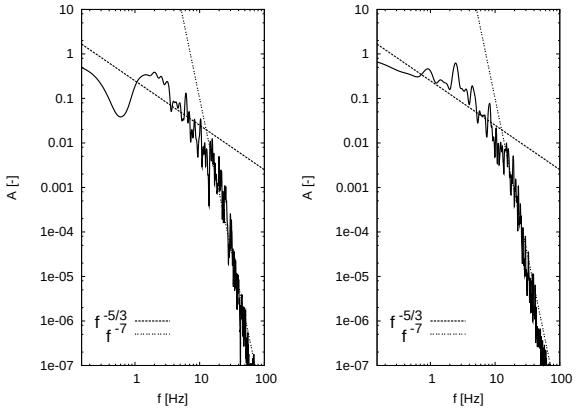

Figure 9: FFT spectra from LES data of $\overline{u}_1$ in PM1 (left) and $\overline{u}_2$ in PM2 (right)

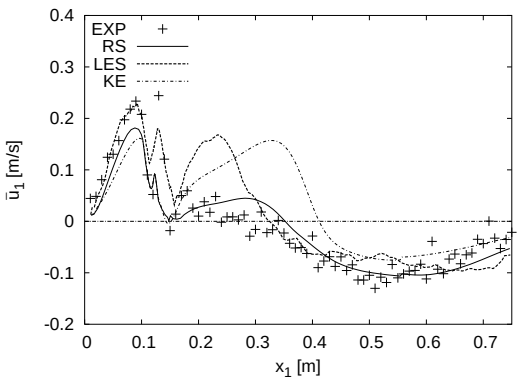

Figure 10: velocity profile $\overline{u}_{1,m}$ at $x_2 = 125\,mm$ and $x_3 = 100\,mm$

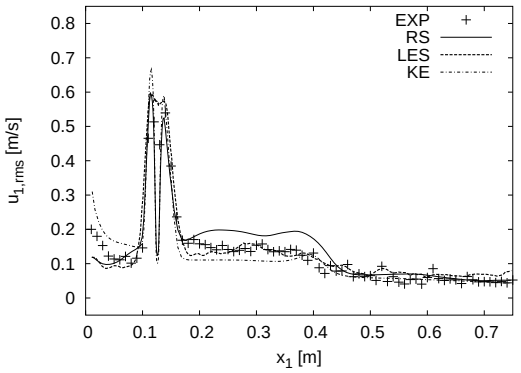

Figure 11: velocity profile $u_{1,rms}$ at $x_2 = 125\,mm$ and $x_3 = 100\,mm$

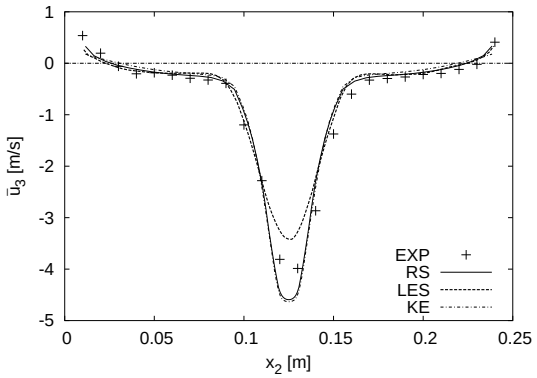

Figure 12: velocity profile $\overline{u}_{3,m}$ at $x_1 = 125\,mm$ and $x_3 = 100\,mm$

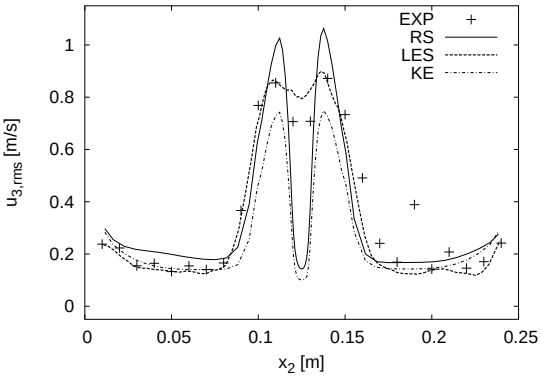

Figure 13: velocity profile $u_{3,rms}$ at $x_1 = 125\,mm$ and $x_3 = 100\,mm$